International Journal of Mathematics and Computer Research

ISSN: 2320-7167

Volume 11 Issue 09 September 2023, Page no. 3765-3779

Index Copernicus ICV: 57.55, Impact Factor: 7.362

DOI: 10.47191/ijmcr/v11i9.10

Viscosity and Hall Effects on Unsteady MHD Casson Fluid Flow through a Parallel Porous Plate

E.O. Anyanwu[1], D. Raymond[2]

[1,2] Federal University Wukari, Wukari, Taraba State, Nigeria

ARTICLE INFO

Published Online:
22 September 2023

ABSTRACT

This study investigates the temperature viscosity and Hall effects of a Casson fluid flow through a porous medium of a viscous incompressible fluid bounded by two parallel porous plates under the influence of thermal radiation and chemical reaction. A uniform suction and injection are applied perpendicular to the plates while the fluid motion is subjected to variable pressure gradient. The transformed conservation equations are solved analytically subject to physically appropriate boundary conditions by using perturbation and Eigenfunction expansion techniques. The influence of a number of emerging non-dimensional parameters namely, variable pressure gradient parameter, suction parameter, radiation parameter and Hartman number are examined. It is observed that the primary velocity profile is increased with increasing temperature dependent viscosity while increase in Hall parameter leads to increase in secondary velocity profile of the flow.

Corresponding Author:
E.O. Anyanwu

KEYWORDS: Perturbation method, MHD, Viscosity, Suction, Hall current.

1. INTRODUCTION

Mathematical Models are used to examine different phenomena with each model representing a definite schematization of the phenomenon taken into consideration. In modeling, the researcher is always restricted by a finite number of parameters called the governing factors within the limits of which the investigation is being carried out. In fluid dynamics, Couette flow is the laminar flow of a viscous fluid in the space between two parallel plates one of which is moving at a velocity relative to the other. The flow is driven by the virtue of viscous drag force acting on the fluid and the applied pressure gradient parallel to the plates. The study of magnetohydrodynamic (MHD) Couette flow with heat transfer of an electrically conducting fluid through two parallel plates known as Hartman flow is a classical problem that has many applications in MHD power generators, MHD pumps, aerodynamic heating, nuclear reactors and geothermal energy extractions. Fluid flow through porous media has several engineering and geophysical applications such as in the field of chemical engineering for filtration and purification processes, in agricultural engineering to study the underground water resources, in petroleum industry to study the movement of natural gas, oil and water through the oil channels and reservoirs while in astrophysics it is applied to study the stellar and solar structures. The most important non-Newtonian fluid possessing a yield value is the Casson fluid, which has significant applications in polymer processing industries and biomechanics. Casson fluid is shear thinning liquid which has an infinite velocity at a zero rate of strain. Cassons constitute equation represents a nonlinear relationship between the rates of stress and strain and has been noticed to be accurately applicable in silicon suspensions and lithographic varnishes used for printing inks. Ajibade and Bichi [1] investigated the variable fluid properties and thermal radiation effects on natural convection Couette flow through a vertical porous channel using the Adomian decomposition method (ADM) and maintained that both fluid velocity and its temperature within the channel were observed to increase with growing thermal radiation and decreases with increase in thermal conduction of the fluid. Yusuf *et al.* [2] examined the boundary layer flow of a nanofluid in an inclined wavy wall with convective boundary condition. They observed fluid flow back at the wavy wall. Anyanwu *et al.* [3] studied the radiative effects on unsteady MHD Couette flow through a parallel plate with constant pressure gradient. Aiyesimi *et al.* [4] analytically investigated the convective boundary layer flow of a nanofluid past a stretching sheet with radiation. They solved

the governing equations using the Adomain decomposition method (ADM). They observed that both thermal and concentration Grashof numbers enhance the velocity, temperature and concentration profiles of the fluid. Laila and Marwat [5] examined the nanofliud flow in a converging and diverging channel of rectangular heated walls. They deduced that both the temperature and concentration profiles are enhanced with increase in thermophoretic forces. Recently, Jiya *et al.* [6] studied using the Adomain decomposition method the solutions of a boundary layer flow past a stretching plate with heat transfer, viscous dissipation and Grashof number. They observed that ADM provides highly precise numerical solution for non-linear differential equations. Chutia *et al.* [7] numerically studied the solution of unsteady hydromagnetic Couette flow in a rotating system bounded by two porous plates with Hall effects. The governing equations were solved using the finite difference method. Jana *et al.* [8] investigated Couette flow through a porous medium in a rotating system and observed that a thin boundary layer which increases in thickness as porosity parameter increases is formed near the moving plate. In another related work, Seth *et al.* [9] studied using Laplace transform technique, the effects of rotation and magnetic field on unsteady Couette flow in a porous channel. They observed that magnetic field retards the fluid flow in both primary and secondary flow directions. Seth *et al.* [10] studied the unsteady hydromagnetic Couette flow within porous plates in a rotating system. They observed that suction has a retarding influence on both the primary and secondary flow where as injection and time have accelerating influence on the flow velocities. Casson fluid as an example of non-Newtonian fluid is a shear thinning liquid with an infinite viscosity at a zero rate of strain. It is an important fluid in mechanics due to its practical applications such as in silicon suspension and suspensions of bentonic in water. Pramanik [11] focused on Casson fluid flow and heat transfer past an exponentially porous stretching surface in the presence of thermal radiation. Afikuzzaman *et al.* [12] have investigated an unsteady MHD Casson fluid flow through a parallel plate with hall current using an explicit finite difference technique. In another related research, hydrodynamic impulsive lid driven flow and heat transfer of a Casson fluid was studied by Attia & Sayed-Ahmed (2006). Sayed-Ahmed *et al.* [13] investigated time dependent pressure gradient effect on unsteady MHD Couette flow of an electrically conducting, viscous, incompressible fluid bounded by two parallel non-conducting porous plates with heat transfer under exponential decaying pressure gradient. Olayiwola [14] investigated the modeling and simulation of combustion fronts in porous media. Jana *et al.* [15] examined Couette flow through a porous medium in a rotating system. In another related work, Seth *et al.* [16] studied the effects of rotation and magnetic field on unsteady Couette flow in a porous channel. Seth *et al.* [17] studied the unsteady hydromagnetic Couette flow within porous plates in a rotating system. Recently, Sharma & Yadav [18] considered Heat transfer through three dimensional Couette flow between a stationary porous plate bounded by porous medium and moving porous plates. Sharma *et al.* [19] investigated the steady laminar flow and heat transfer of a non-Newtonian fluid through a straight horizontal porous channel in the presence of heat source.

2. MATHEMATICAL FORMULATION

Following Anyanwu *et al.* [3] while they analyzed the flow under constant pressure gradient, the unsteady flow of a viscous, incompressible, non-conducting fluid through a channel with chemical reaction and thermal radiation in the presence of magnetic field is investigated under a time/temperature dependent pressure gradient. The flow is assumed to be laminar, incompressible and flows between two infinite horizontal plates located at $y = \pm h$ which extends from $x = -\infty$ to ∞ and from $z = -\infty$ to ∞.

The upper plate is suddenly set into motion and moves with a uniform velocity U_0 while the lower plate is kept stationary as shown in the diagram below. The upper plate is simultaneously subjected to a step change in temperature from T_1 to T_2. The upper and lower plates are kept at two constant temperatures T_2 and T_1 respectively with $T_2 > T_1$. The fluid flows between the two plates under the influence of an exponential decaying with time pressure gradient in the x-direction which is a generalization of a constant pressure gradient. A uniform suction from above and injection from below with constant velocity v_0 which are all applied at $t = 0$. The system is subjected to a uniform magnetic field B_0 in the positive y-direction and is assumed undisturbed as the induced magnetic field is neglected by assuming a small magnetic Reynolds number. The Hall effect is taken into consideration and consequently a z-component of the velocity is expected to arise.

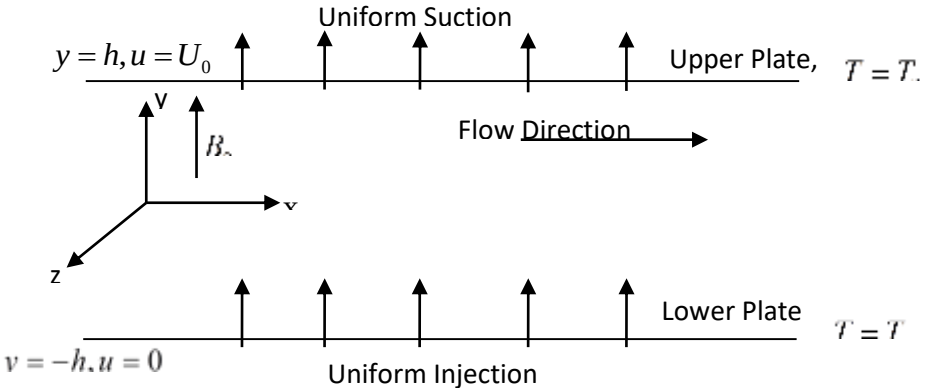

Figure 1: Schematic diagram of the problem

Based on the above assumptions,

$$v = ui + v_0 j + wk \tag{1}$$

Introducing a Chapman-Rubesin viscosity law, with $w = 1$ as shown in Olayiwola (2016) and using the condition at the lower plate, results in:

$$\mu = \frac{c\mu_1 T}{T_1} \tag{2}$$

Where μ_1 is the Casson coefficient of viscosity.

Thus, the two components of the governing momentum equation in dimensional form are as follows:

$$\rho\frac{\partial u}{\partial t} + \rho v_0 \frac{\partial u}{\partial y} = -\frac{\partial p}{\partial x} + \frac{\partial}{\partial y}\left(\mu\frac{\partial u}{\partial y}\right) - \frac{\sigma B_0^2}{(1+BiBe)^2 + Be^2}\left[(1+BiBe)u + Bew\right] -$$

$$\mu\frac{u}{k} + g\beta_T\left(T - T_1\right) + g\beta_C\left(C - C_1\right) \tag{3}$$

$$\rho\frac{\partial w}{\partial t} + \rho v_0 \frac{\partial w}{\partial y} = \frac{\partial}{\partial y}\left(\mu\frac{\partial w}{\partial y}\right) - \frac{\sigma B_0^2}{(1+BiBe)^2 + Be^2}\left[(1+BiBe)w - Beu\right] - \mu\frac{w}{k} \tag{4}$$

The energy equation in dimensional form is given as

$$\left.\begin{aligned}\rho C_P\frac{\partial T}{\partial t} + \rho C_P v_0\frac{\partial T}{\partial y} = \frac{1}{\Pr}\frac{\partial}{\partial y}\left(\mu\frac{\partial T}{\partial y}\right) + \mu\left[\left(\frac{\partial u}{\partial y}\right)^2 + \left(\frac{\partial w}{\partial y}\right)^2\right] + \\ \frac{\sigma B_0^2}{(1+BiBe)^2 + Be^2}\left[u^2 + w^2\right] - \frac{1}{\rho C_P}\frac{\partial q}{\partial y}\end{aligned}\right\} \tag{5}$$

The concentration equation in dimensional form is given as:

$$\rho\frac{\partial C}{\partial t} + \rho v_0\frac{\partial C}{\partial y} = \frac{1}{Sc}\frac{\partial}{\partial y}\left(\mu\frac{\partial C}{\partial y}\right) + D_1\frac{\partial^2 T}{\partial y^2} - D_2\left(C_2 - C_1\right) \tag{6}$$

Subject to the initial and boundary conditions;

$$\left.\begin{array}{lll} u(y,0)=0, & u(-h,t)=0, & u(h,t)=U_0 \\ w(y,0)=U_0 y(1-y), & w(-h,t)=0, & w(h,t)=0 \\ T(y,0)=0, & T(-h,t)=T_1, & T(h,t)=T_2 \\ C(y,0)=0, & C(-h,t)=C_1, & C(h,t)=C_2 \end{array}\right\} \qquad (7)$$

Where ρ and μ are respectively the density and apparent viscosity of the fluid, σ is electric conductivity, β is Hall factor, Bi is ion slip parameter, $Be=\sigma\beta B_0$ is Hall parameter, c and k are respectively the specific heat capacity and thermal conductivity of the fluid. Where u and w are components of velocities along and perpendicular to the plate in x and y directions respectively, σ is the electrical conductivity, β_T is the coefficient of volume expansion of the moving fluid, β_C is the coefficient of volumetric expansion with concentration, v is the kinematic viscosity, T is the temperature of the fluid, C is the concentration of the fluid, C_1 is concentration at infinity, D_1 the thermal diffusivity, D_2 the chemical reaction rate constant, C_P is the specific heat capacity at constant pressure. t is time, g is gravitational force, μ_e is magnetic permeability of the fluid, K is the porous media permeability coefficient, q is radiative heat flux, H_0 is intensity of magnetic field, $B_0=\mu_e H_0$ is electromagnetic induction, τ_0 is yield stress, β is coefficient of volume expansion due to temperature and α is mean radiation absorption coefficient.

To write the governing dimensional equations (3)-(6) with their corresponding boundary conditions (7) in non-dimensional form, we use the following dimensionless variables:

$$\bar{u}=\frac{u}{U_0}, \qquad \bar{w}=\frac{w}{U_0}, \qquad \bar{y}=\frac{y}{h}, \qquad \bar{x}=\frac{x}{h}, \qquad \bar{t}=\frac{tU_0}{h}, \qquad \theta=\frac{T-T_1}{T_2-T_1} \qquad (8)$$

$$\phi=\frac{C-C_1}{C_2-C_1}, \qquad \bar{P}=\frac{P}{\rho U_0^2}, \qquad \bar{\mu}=\frac{c\mu_1 T}{T_1}$$

and we obtain

When the pressure gradient is a function of time: $\frac{\partial p}{\partial x}=\frac{dp}{dx}=-\lambda e^{-\varepsilon t}$ (9)

In this case, equations (3) - (6) reduce to;

$$\frac{\partial u}{\partial t}+\frac{S}{2}\frac{\partial u}{\partial z}=-\lambda e^{-\varepsilon t}+\frac{c}{4\,\mathrm{Re}}\frac{\partial}{\partial z}\left((1+\alpha\theta)\frac{\partial u}{\partial z}\right)-\frac{Ha^2}{\mathrm{Re}\left((1+BiBe)^2+Be^2\right)}\left((1+BiBe)^2u+Be^2w\right)- \qquad (10)$$

$$\frac{cP}{\mathrm{Re}}(\alpha\theta+1)u+Gr_\theta\theta+Gr_\phi\phi$$

$$\frac{\partial w}{\partial t}+\frac{S}{2}\frac{\partial w}{\partial z}=\frac{c}{4\,\mathrm{Re}}\frac{\partial}{\partial z}\left((1+\alpha\theta)\frac{\partial w}{\partial z}\right)-\frac{Ha^2}{\mathrm{Re}\left((1+BiBe)^2+Be^2\right)}\left((1+BiBe)^2w-Be^2u\right)- \qquad (11)$$

$$\frac{cP}{\mathrm{Re}}(\alpha\theta+1)w$$

$$\frac{\partial\theta}{\partial t}+\frac{S}{2}\frac{\partial\theta}{\partial z}=\frac{c}{4\,\mathrm{Re}\,\mathrm{Pr}}\frac{\partial}{\partial z}\left((1+\alpha\theta)\frac{\partial\theta}{\partial z}\right)+\frac{cEc}{4\,\mathrm{Re}}(1+\alpha\theta)\left(\left(\frac{\partial u}{\partial z}\right)^2+\left(\frac{\partial w}{\partial z}\right)^2\right)+ \qquad (12)$$

$$\frac{EcHa^2}{\mathrm{Re}\left((1+BiBe)^2+Be^2\right)}\left(u^2+w^2\right)-Ra^2\theta$$

$$\frac{\partial \phi}{\partial t}+\frac{S}{2}\frac{\partial \phi}{\partial z}=\frac{c}{4Sc\,\mathrm{Re}}\frac{\partial}{\partial z}\left(\left(1+\alpha\theta\right)\frac{\partial \phi}{\partial z}\right)+\frac{T_D}{4}\frac{\partial^2\theta}{\partial z^2}-K_r\phi \tag{13}$$

Subject to the initial and boundary conditions

$$\left.\begin{array}{lll} u(y,0)=0, & u(-1,t)=0, & u(1,t)=1 \\ w(y,0)=y(1-y), & w(-1,t)=0, & w(1,t)=0 \\ \theta(y,0)=0, & \theta(-1,t)=0, & \theta(1,t)=1 \\ \phi(y,0)=0, & \phi(-1,t)=0, & \phi(1,t)=1 \end{array}\right\} \tag{14}$$

Where

$$\left.\begin{array}{llll} \mathrm{Re}=\frac{\rho U_0 h}{\mu_1}, & S=\frac{\nu_0}{U_0}, & P=\frac{h^2\mu_1}{k}, & Ha^2=\frac{\sigma B_0^2 h^2}{\mu_1}, \quad Gr_\theta=\frac{g\beta_T\left(T_2-T_1\right)h}{\rho U_0^2}, \\ Gr_\phi=\frac{g\beta_C\left(C_2-C_1\right)h}{\rho U_0^2}, & \mathrm{Pr}=\frac{\mu_1 c_p}{k}, & Ec=\frac{U_0^2}{c_p\left(T_2-T_1\right)}, & Ra^2=\frac{4\alpha^2 h}{\rho^2 C_p^2 U_0}, \\ Sc=\frac{U_0 h}{D}, & T_D=\frac{D\left(T_2-T_1\right)}{h\left(C_2-C_1\right)U_0}, & \alpha=\frac{T_2-T_1}{T_1}, & Kr=\frac{D_2 h}{\rho U_0}, \end{array}\right\}$$

3. METHOD OF SOLUTION

Since the boundary conditions are from -1 to 1, we first transform the boundary conditions to 0 to 1 using the transformation:

$$z=\frac{y+1}{2} \tag{15}$$

Let $0<\alpha<<1$ such that $Ec=b\alpha, S=e\alpha,\ Be=f\alpha, Gr_\theta=g\alpha, Gr_\phi=l\alpha$ and suppose the solutions of equations (10) – (13) satisfying (14) can be expressed as

$$\left.\begin{array}{l} u(z,t)=u_0(z,t)+\alpha u_1(z,t)+\ldots \\ w(z,t)=w_0(z,t)+\alpha w_1(z,t)+\ldots \\ \theta(z,t)=\theta_0(z,t)+\alpha\theta_1(z,t)+\ldots \\ \phi(z,t)=\phi_0(z,t)+\alpha\phi_1(z,t)+\ldots \end{array}\right\} \tag{16}$$

Therefore, the equations for $u_0, w_0, \theta_0, \phi_0, u_1, w_1, \theta_1$ and ϕ_1 together with their initial and boundary conditions are given by

$$\left.\begin{array}{l} \frac{\partial\theta_0}{\partial t}=\frac{c}{4\,\mathrm{Re}\,\mathrm{Pr}}\frac{\partial}{\partial z}\left(\frac{\partial\theta_0}{\partial z}\right)-Ra^2\theta_0 \\ \theta_0(z,0)=d_1, \quad \theta_0(0,t)=0, \quad \theta_0(1,t)=1 \end{array}\right\} \tag{17}$$

$$\left.\begin{array}{l} \frac{\partial\phi_0}{\partial t}=\frac{c}{4Sc\,\mathrm{Re}}\frac{\partial}{\partial z}\left(\frac{\partial\phi_0}{\partial z}\right)+T_D\frac{\partial^2\theta_0}{\partial z^2}-K_r\phi_0 \\ \phi_0(z,0)=d_2, \quad \phi_0(0,t)=0, \quad \phi_0(1,t)=1 \end{array}\right\} \tag{18}$$

$$\left.\begin{aligned}&\frac{\partial w_0}{\partial t}=\frac{c}{4\,\mathrm{Re}}\frac{\partial}{\partial z}\left(\frac{\partial w_0}{\partial z}\right)-\frac{Ha^2}{\mathrm{Re}}w_0-\frac{cP}{\mathrm{Re}}w_0\\&w_0(z,0)=(2z-1)(2-2z),\quad w_0(0,t)=0,\quad w_0(1,t)=0\end{aligned}\right\}\tag{19}$$

$$\left.\begin{aligned}&\frac{\partial u_0}{\partial t}=\frac{c}{4\,\mathrm{Re}}\frac{\partial}{\partial z}\left(\frac{\partial u_0}{\partial z}\right)-\frac{Ha^2}{\mathrm{Re}}u_0-\frac{cP}{\mathrm{Re}}(u_0)-\lambda e^{-\varepsilon t}\\&u_0(z,0)=0,\quad u_0(0,t)=0,\quad u_0(1,t)=1\end{aligned}\right\}\tag{20}$$

$$\left.\begin{aligned}&\frac{\partial u_1}{\partial t}+\frac{e}{2}\frac{\partial u_0}{\partial z}=\frac{c}{4\,\mathrm{Re}}\frac{\partial}{\partial z}\left(\frac{\theta_0\partial u_0}{\partial z}+\frac{\partial u_1}{\partial z}\right)-\frac{Ha^2}{\mathrm{Re}}(-Bifu_0+u_1+fw_0)-\frac{cP}{\mathrm{Re}}(\theta_0u_0+u_1)+\\&g\theta_0+l\phi_0\\&u_1(z,0)=0,\qquad u_1(0,t)=0,\qquad u_1(1,t)=0\end{aligned}\right\}\tag{21}$$

$$\left.\begin{aligned}&\frac{\partial\theta_1}{\partial t}+\frac{e}{2}\frac{\partial\theta_0}{\partial z}=\frac{c}{4\,\mathrm{Re}\,\mathrm{Pr}}\frac{\partial}{\partial y}\left(\theta_0\frac{\partial\theta_0}{\partial z}+\frac{\partial\theta_1}{\partial z}\right)+\frac{bc}{4\,\mathrm{Re}}\left(\left(\frac{\partial u_0}{\partial z}\right)^2+\left(\frac{\partial w_0}{\partial z}\right)^2\right)-\\&\frac{bHa^2}{\mathrm{Re}}\left((u_0)^2+(w_0)^2\right)-Ra^2\theta_1\\&\theta_1(z,0)=0,\qquad \theta_1(0,t)=0,\qquad \theta_1(1,t)=0\end{aligned}\right\}\tag{22}$$

$$\left.\begin{aligned}&\frac{\partial w_1}{\partial t}+\frac{e}{2}\frac{\partial w_0}{\partial z}=\frac{c}{4\,\mathrm{Re}}\frac{\partial}{\partial z}\left(\theta_0\frac{\partial w_0}{\partial z}+\frac{\partial w_1}{\partial z}\right)-\frac{Ha^2}{\mathrm{Re}}(-Bifw_0+w_1-fu_0)-\frac{cP}{\mathrm{Re}}(\theta_0w_0+w_1)\\&w_1(z,0)=0,\qquad w_1(0,t)=0,\qquad w_1(1,t)=0\end{aligned}\right\}\tag{23}$$

$$\left.\begin{aligned}&\frac{\partial\phi_1}{\partial t}+\frac{e}{2}\frac{\partial\phi_0}{\partial z}=\frac{c}{4Sc\,\mathrm{Re}}\frac{\partial}{\partial z}\left(\theta_0\frac{\partial\phi_0}{\partial z}+\frac{\partial\phi_1}{\partial z}\right)+T_D\frac{\partial^2\theta_1}{\partial z^2}-K_r\phi_1\\&\phi_1(z,0)=0,\qquad \phi_1(0,t)=0,\qquad \phi_1(1,t)=0\end{aligned}\right\}\tag{24}$$

Eigenfunction Expansion Technique

Now, consider the problem (see Myint-U and Debnath, (1987))

$$\left.\begin{aligned}&\frac{\partial u}{\partial t}=k\frac{\partial^2u}{\partial x^2}+\alpha u+F(x,t)\\&u(x,0)=f(x),\qquad u(0,t)=0,\qquad u(L,t)=0\end{aligned}\right\}\tag{25}$$

For problem (25) above, we assume a solution of the form

$$u(x,t)=\sum_{n=1}^{\infty}u_n(t)\sin\frac{n\pi}{L}x\tag{26}$$

Where

$$u_n(t)=\int_0^t e^{\left(\alpha-k\left(\frac{n\pi}{L}\right)^2\right)(t-\tau)}F_n(\tau)d\tau+b_n e^{\left(\alpha-k\left(\frac{n\pi}{L}\right)^2\right)t} \quad (27)$$

$$F_n(t)=\frac{2}{L}\int_0^L F(x,t)\sin\frac{n\pi}{L}xdx \quad (28)$$

$$b_n(t)=\frac{2}{L}\int_0^L F(x)\sin\frac{n\pi}{L}xdx \quad (29)$$

Comparing equation (17) – (24) with the (25) we obtain the solutions to the velocity (primary and secondary), temperature, and concentration distributions as

$$\theta_0(\mathrm{z},\mathrm{t})=\mathrm{z}+\sum_{n=1}^{\infty}\left(q_1+\left(b_n-q_1\right)e^{-q_0t}\right)\sin n\pi z \quad (30)$$

$$\phi_0(z,t)=z+\sum_{n=1}^{\infty}\left(q_3\left(1-e^{-q_2t}\right)-\sum_{n=1}^{\infty}\left(q_4-q_5e^{-q_2t}+q_6e^{-q_0t}\right)+b_{2n}e^{-q_2t}\right)\sin n\pi z \quad (31)$$

$$w_0(\mathrm{z},t)=\sum_{n=1}^{\infty}b_{3n}e^{-q_8t}Sinn\pi z \quad (32)$$

$$u_0\left(z,t\right)=z+\sum_{n=1}^{\infty}\left(q_9+q_{10}e^{-q_8t}+q_{11}e^{-\varepsilon t}\right)\sin n\pi z \quad (33)$$

Where $q_9=\frac{2q_7(-1)^n}{n\pi q_8}$, $q_{10}=\left(b_n-\frac{2q_7(-1)^n}{n\pi q_8}-\frac{\sigma\left((-1)^n-1\right)}{n\pi\left(q_8-\varepsilon\right)}\right)$, $q_{11}=\frac{\sigma\left((-1)^n-1\right)}{n\pi\left(q_8-\varepsilon\right)}$

$$u_1\left(z,t\right)=\sum_{n=1}^{\infty}v_{5n}\left(t\right)\sin n\pi z \quad (34)$$

Where

$$v_{5n}\left(t\right)=2\left(\begin{array}{l}\frac{q_{15}}{q_8}\left(1-e^{q_8t}\right)+\sum_{n=1}^{\infty}\left(\begin{array}{l}\frac{q_{16}}{q_8}\left(1-e^{-q_8t}\right)+q_{17}te^{-q_8t}+\frac{q_{18}}{\left(q_8-\varepsilon\right)}\left(e^{-\varepsilon t}-e^{-q_8t}\right)+\\ \frac{q_{19}}{\left(q_8-q_0\right)}\left(e^{-q_0t}-e^{-q_8t}\right)+\frac{q_{20}}{\left(q_8-q_2\right)}\left(e^{-q_2t}-e^{-q_8t}\right)\end{array}\right)+\\ \sum_{n=1}^{\infty}\sum_{n=1}^{\infty}\left(\begin{array}{l}\frac{q_{21}}{q_8}\left(1-e^{-q_8t}\right)+q_{22}te^{-q_8t}+\frac{q_{23}}{\left(q_8-\varepsilon\right)}\left(e^{-\varepsilon t}-e^{-q_8t}\right)+\frac{q_{24}}{\left(q_8-q_0\right)}\left(e^{-q_0t}-e^{-q_8t}\right)-\\ \frac{q_{25}}{q_0}\left(e^{-(q_8+q_0)t}-e^{-q_8t}\right)+\frac{q_{26}}{\left(q_8-q_0-\varepsilon\right)}\left(e^{-(q_0+\varepsilon)t}-e^{-q_8t}\right)+\frac{q_{27}}{\left(q_8-q_2\right)}\left(e^{-q_2t}-e^{-q_8t}\right)\end{array}\right)\end{array}\right)$$

$$\theta_1\left(z,t\right)=\sum_{n=1}^{\infty}v_{6n}\left(t\right)Sinn\pi z \quad (35)$$

Where

$$v_{6n}(t)=2\left(\begin{array}{l} q_{31}\left(1-e^{-q_0 t}\right)+ \\ \sum_{n=1}^{\infty}\left(q_{48}\left(1-e^{-q_0 t}\right)+q_{49}te^{-q_0 t}+q_{50}\left(e^{-q_8 t}-e^{-q_0 t}\right)-q_{51}\left(e^{-\varepsilon t}-e^{-q_0 t}\right)\right)+ \\ \sum_{n=1}^{\infty}\sum_{n=1}^{\infty}\left(\begin{array}{l} q_{39}\left(1-e^{-q_0 t}\right)+q_{40}\left(e^{-q_8 t}-e^{-q_0 t}\right)+q_{41}\left(e^{-\varepsilon t}-e^{-q_0 t}\right)+q_{42}\left(e^{-2q_8 t}-e^{-q_0 t}\right)+ \\ q_{43}\left(e^{-(q_8+\varepsilon)t}-e^{-q_0 t}\right)+q_{44}\left(e^{-2\varepsilon t}-e^{-q_0 t}\right) \end{array}\right) \end{array}\right)$$

$$w_1(z,t)=\sum_{n=1}^{\infty}v_{7n}(t)\sin n\pi z \tag{36}$$

Where

$$v_{7n}(t)=2\left(\begin{array}{l} -\frac{Ha^2 f(-1)^n}{n\pi\,\mathrm{Re}\,q_8}\left(1-e^{-q_8 t}\right)+\sum_{n=1}^{\infty}\left(\begin{array}{l} \frac{Ha^2 fq_9}{2\,\mathrm{Re}\,q_8}\left(1-e^{-q_8 t}\right)+\left(\begin{array}{l} \frac{Ha^2 f}{2\,\mathrm{Re}}\left(q_{10}+Bib_{3n}\right)+\frac{q_{12}b_{3n}\left(1-(-1)^{2n}\right)}{2}- \\ b_{3n}\frac{\left(1+n^2\pi^2-(-1)^{2n}\right)}{4(n\pi)^2}\left(\frac{c(n\pi)^2}{4\,\mathrm{Re}}+\frac{cP}{\mathrm{Re}}\right) \end{array}\right)te^{-q_8 t}+ \\ \frac{Ha^2 fq_9}{2\,\mathrm{Re}\left(q_8-\varepsilon\right)}\left(e^{-\varepsilon t}-e^{-q_8 t}\right) \end{array}\right)+ \\ \sum_{n=1}^{\infty}\sum_{n=1}^{\infty}\left(\begin{array}{l} \frac{b_{3n}\left((-1)^{3n}-3(-1)^n+2\right)}{3n\pi}\left(\frac{c(n\pi)^2}{4\,\mathrm{Re}}+\frac{cP}{\mathrm{Re}}\right)+ \\ b_{3n}\left(\frac{c(n\pi)^2}{4\,\mathrm{Re}}\left(\frac{1-(-1)^{3n}}{3n\pi}\right)-\frac{cP\left((-1)^{3n}-3(-1)^n+2\right)}{3n\pi\,\mathrm{Re}}\right) \end{array}\right)\left(q_1te^{-q_8 t}+\frac{(b_n-q_1)}{q_0}\left(e^{-(q_0+q_8)t}-e^{-q_8 t}\right)\right) \end{array}\right)$$

$$\phi_1(z,t)=\sum_{n=1}^{\infty}v_{8n}(t)\sin n\pi z \tag{37}$$

Where

$$v_{8n}(t)=2\left(\begin{array}{l} \frac{q_{53}}{q_2}\left(1-e^{-q_2 t}\right)+\sum_{n=1}^{\infty}\left(\begin{array}{l} \frac{q_{54}}{q_2}\left(1-e^{-q_2 t}\right)+\frac{q_{53}}{(q_2-q_0)}\left(e^{-q_0 t}-e^{-q_2 t}\right)- \\ 2q_{56}\left(\begin{array}{l} \frac{q_{31}}{q_2}\left(1-e^{-q_2 t}\right)-\frac{q_{31}}{(q_2-q_0)}\left(e^{-q_0 t}-e^{-q_2 t}\right)+ \\ \sum_{n=1}^{\infty}\frac{q_{48}}{q_0}\left(1-e^{-q_2 t}\right)-\frac{q_{48}}{(q_2-q_0)}\left(e^{-q_0 t}-e^{-q_2 t}\right)+q_{49}\left(\frac{te^{-q_0 t}}{(q_2-q_0)}-\frac{\left(e^{-q_0 t}-e^{-q_2 t}\right)}{(q_2-q_0)^2}\right)+ \\ \frac{q_{50}}{(q_2-q_8)}\left(e^{-q_8 t}-e^{-q_2 t}\right)-\frac{q_{50}}{(q_2-q_0)}\left(e^{-q_0 t}-e^{-q_2 t}\right)+\frac{q_{51}}{(q_2-\varepsilon)}\left(e^{-\varepsilon t}-e^{-q_2 t}\right)- \\ \frac{q_{51}}{(q_2-q_0)}\left(e^{-q_0 t}-e^{-q_2 t}\right)+ \end{array}\right) \end{array}\right)+ \\ \sum_{n=1}^{\infty}\sum_{n=1}^{\infty}\left(\begin{array}{l} \frac{q_{39}}{q_2}\left(1-e^{-q_2 t}\right)-\frac{q_{39}}{(q_2-q_0)}\left(e^{-q_0 t}-e^{-q_2 t}\right)+\frac{q_{40}}{(q_2-q_8)}\left(e^{-q_8 t}-e^{-q_2 t}\right)\Big)-\frac{q_{40}}{(q_2-q_0)}\left(e^{-q_0 t}-e^{-q_2 t}\right)- \\ \frac{q_{41}}{(q_2-\varepsilon)}\left(e^{-\varepsilon t}-e^{-q_2 t}\right)-\frac{q_{41}}{(q_2-q_0)}\left(e^{-q_0 t}-e^{-q_2 t}\right)+\frac{q_{42}}{(q_2-2q_8)}\left(e^{-2q_8 t}-e^{-q_2 t}\right)-\frac{q_{42}}{(q_2-q_0)}\left(e^{-q_0 t}-e^{-q_2 t}\right)+ \\ \frac{q_{43}}{(q_2-(q_8+\varepsilon))}\left(e^{-(q_8+\varepsilon)t}-e^{-q_2 t}\right)-\frac{q_{43}}{(q_2-q_0)}\left(e^{-q_0 t}-e^{-q_2 t}\right)+\frac{q_{44}}{(q_2-2\varepsilon)}\left(e^{-2\varepsilon t}-e^{-q_2 t}\right)-\frac{q_{44}}{(q_2-q_0)}\left(e^{-q_0 t}-e^{-q_2 t}\right) \end{array}\right) \\ \sum_{n=1}^{\infty}\left(\left(\frac{q_{57}}{q_2}\left(1-e^{-q_2 t}\right)+q_{58}te^{-q_2 t}-\sum_{n=1}^{\infty}\frac{q_{59}}{q_2}\left(1-e^{-q_2 t}\right)-q_{60}te^{-q_2 t}+\frac{q_{61}}{(q_2-q_0)}\left(e^{-q_0 t}-e^{-q_2 t}\right)\right)+\left(\frac{q_{62}}{q_2}\left(1-e^{-q_2 t}\right)+\frac{q_{63}}{(q_2-q_0)}\left(e^{-q_0 t}-e^{-q_2 t}\right)\right)-\right. \\ \left.\sum_{n=1}^{\infty}\left(\frac{q_{64}}{q_2}\left(1-e^{-q_2 t}\right)+q_{65}te^{-q_2 t}-\sum_{n=1}^{\infty}\left(\frac{q_{66}}{q_2}\left(1-e^{-q_2 t}\right)-q_{67}te^{-q_2 t}+\frac{q_{68}}{(q_2-q_0)}\left(e^{-q_0 t}-e^{-q_2 t}\right)\right)\right)+ \\ \sum_{n=1}^{\infty}\sum_{n=1}^{\infty}\left(\begin{array}{l} \frac{q_{69}}{q_2}\left(1-e^{-q_2 t}\right)+q_{70}te^{-q_2 t}-\sum_{n=1}^{\infty}\left(\frac{q_{71}}{q_2}\left(1-e^{-q_2 t}\right)-q_{72}te^{-q_2 t}+\frac{q_{73}}{(q_2-q_0)}\left(e^{-q_0 t}-e^{-q_2 t}\right)\right)\frac{q_{74}}{(q_2-q_0)}\left(e^{-q_0 t}-e^{-q_2 t}\right)- \\ \frac{q_{75}}{q_0}\left(e^{-(q_2+q_0)t}-e^{-q_2 t}\right)-\sum_{n=1}^{\infty}\left(\frac{q_{76}}{(q_2-q_0)}\left(e^{-q_0 t}-e^{-q_2 t}\right)+\frac{q_{77}}{q_0}\left(e^{-(q_2+q_0)t}-e^{-q_2 t}\right)+\frac{q_{78}}{(q_2-2q_0)}\left(e^{-2q_0 t}-e^{-q_2 t}\right)\right) \end{array}\right) \end{array}\right)$$

Therefore the solutions to the governing equations are given as:

$$\theta(\mathrm{z,t}) = \mathrm{z} + \sum_{n=1}^{\infty}\left(q_1 + \left(b_n - q_1\right)e^{-q_0 t}\right)\sin n\pi z + a\sum_{n=1}^{\infty} v_{6n}(t)\,Sinn\pi z \tag{38}$$

$$\phi(\mathrm{z,t}) = z + \sum_{n=1}^{\infty}\left(q_3\left(1-e^{-q_2 t}\right) - \sum_{n=1}^{\infty}\left(q_4 - q_5 e^{-q_2 t} - q_6 e^{-q_0 t}\right) + b_{2n}e^{-q_2 t}\right)\sin n\pi z + a\sum_{n=1}^{\infty} v_{8n}(t)\,sinn\pi z \tag{39}$$

$$w(\mathrm{z},t) = \sum_{n=1}^{\infty} b_{3n}e^{-q_8 t}\,Sinn\pi z + a\sum_{n=1}^{\infty} v_{7n}(t)\,Sinn\pi z \tag{40}$$

$$u(z,t) = z + \sum_{n=1}^{\infty}\left(q_9 + q_{10}e^{-q_8 t} - q_{11}e^{-\varepsilon t}\right)Sinn\pi z + a\sum_{n=1}^{\infty} v_{5n}(t)\,Sinn\pi z \tag{41}$$

4. RESULTS AND DISCUSSIONS

The system of partial differential equations describing unsteady Couette flow of an electrically conducting incompressible fluid bounded by two parallel non conducting porous plates are solved analytically using eigenfunction expansion method. The analytical solutions of the governing equations are computed and presented graphically with the aid of a computer symbolic algebraic package MAPLE 17 for the values of the following parameters:

$\mathrm{Re} = 1,$ $Ra^2 = 1,$ $S = 0.1,$ $\mathrm{Pr} = 0.71,$ $Ha^2 = 1,$ $Kr = 0.5,$ $Sc = 0.22,$

$Bi = 1,$ $Be = 1,$ $\alpha = 0.1,$ $c = 0.2,$ $P = 1,$ $T_D = 0,$ $Ec = 0.01,$

$\mathrm{Gr}_\theta = 0.2,$ $Gr_\phi = 0.2,$ $\sigma = 2$

The figure 2-12 explains the graphs of primary and secondary velocities, temperature and concentration profiles against different dimensionless parameters.

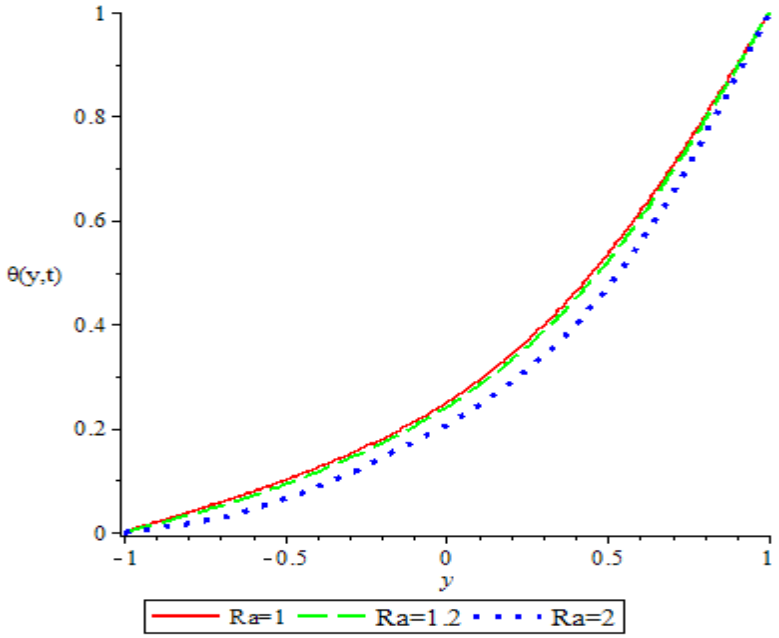

Figure 2: Effect of radiation parameter (Ra) on temperature profile $\theta(y,t)$

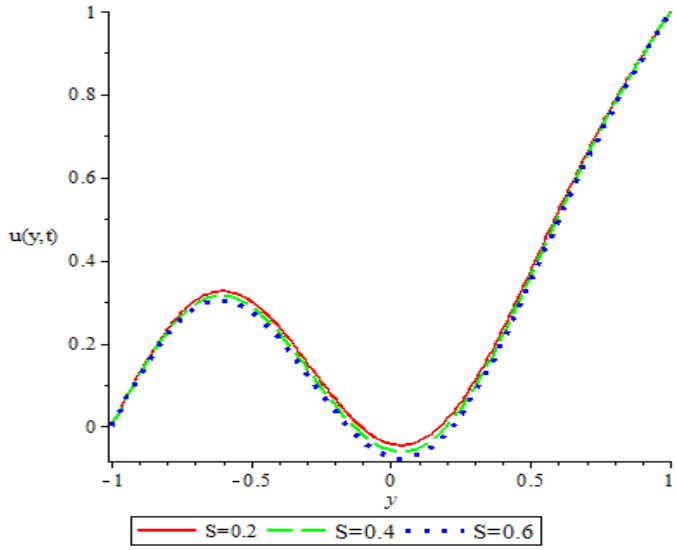

Figure 3: Effect of suction parameter (S) on primary velocity profile $u(y,t)$

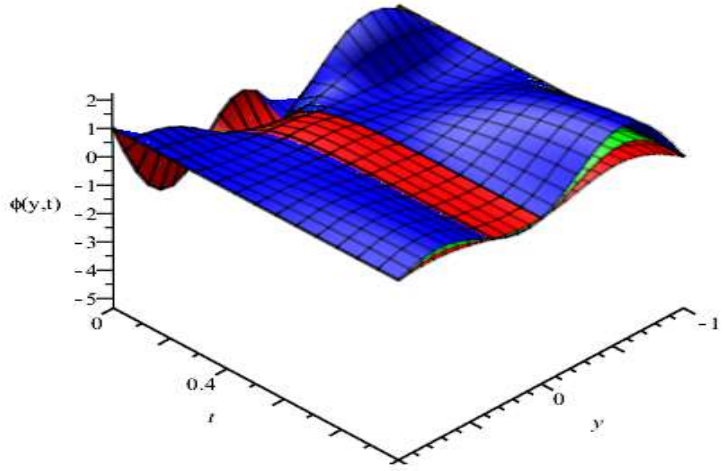

Figure 4: Effect of suction parameter (S) on concentration profile $\phi(y,t)$ along distance y and time t. S=0.2(red), S=0.4(green) and S=0.6(blue)

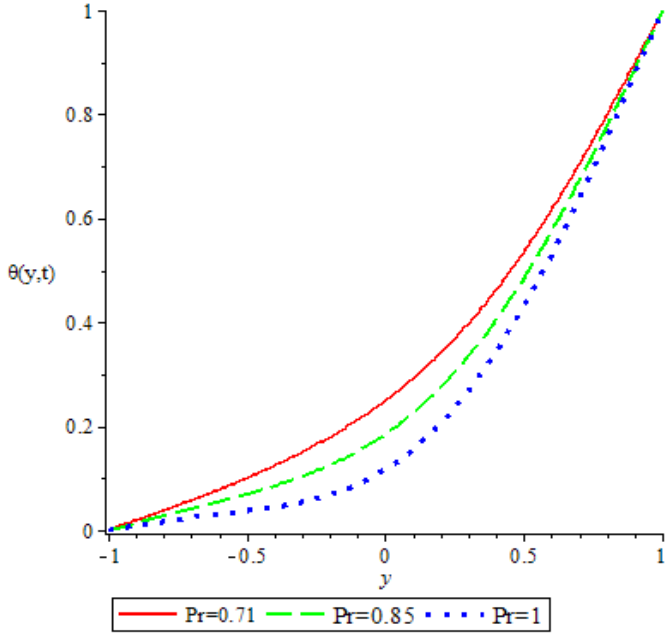

Figure 5: Effect of Prandtl number $(\Pr)$ on temperature profile $\theta(y,t)$

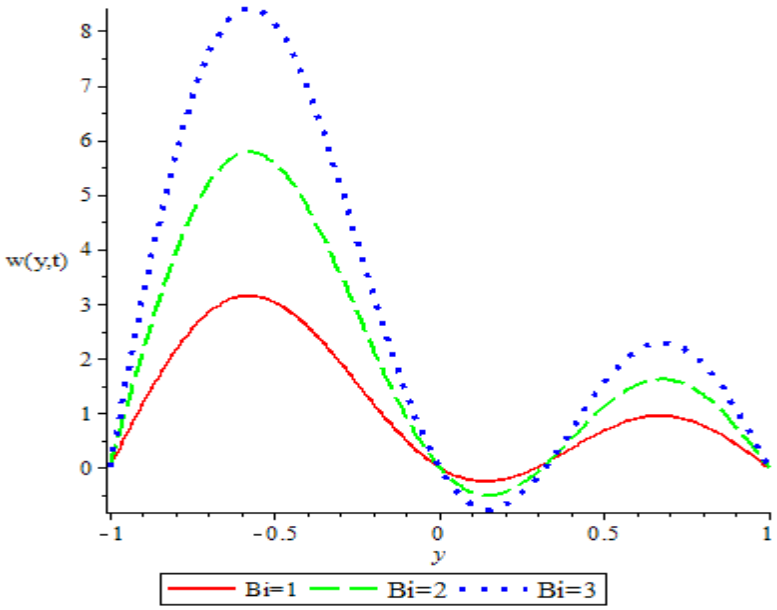

Figure 6: Effect of ion slip parameter (Bi) on secondary velocity profile $w(y,t)$

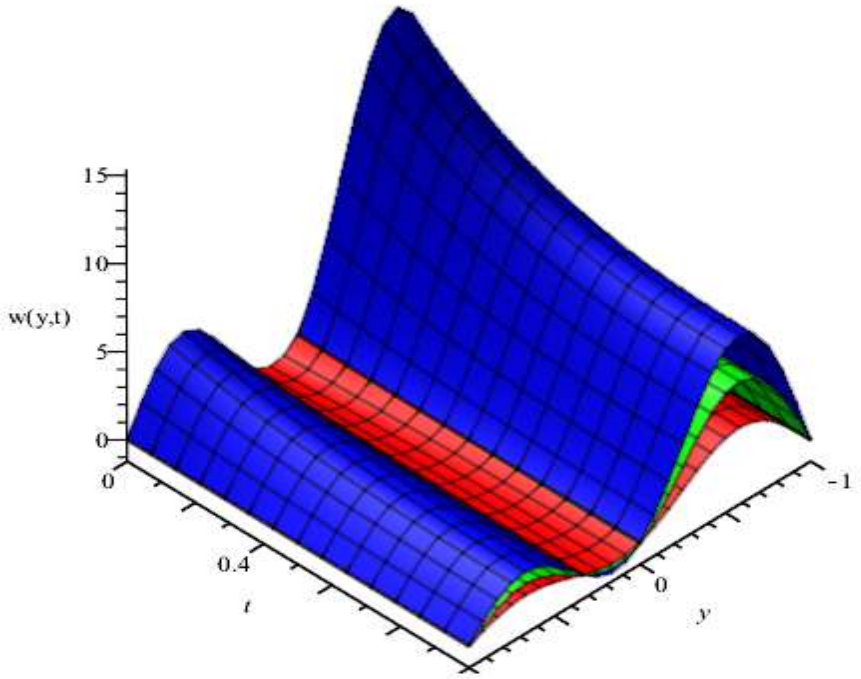

Figure 7: Effect of ion slip parameter (Bi) on secondary velocity profile $w(y,t)$ along distance y and time t. Bi=1(red), Bi=2(green) and Bi=3(blue)

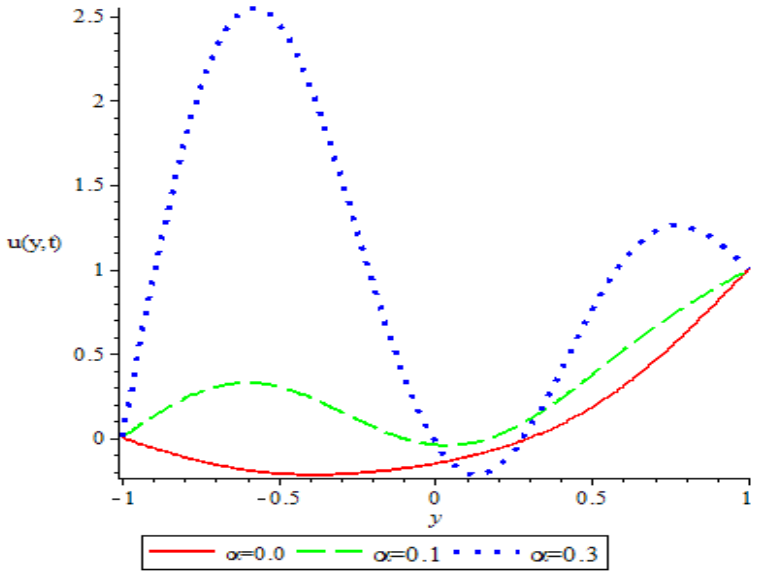

Figure 8: Effect of temperature dependent viscosity (α) on primary velocity profile $u(y,t)$

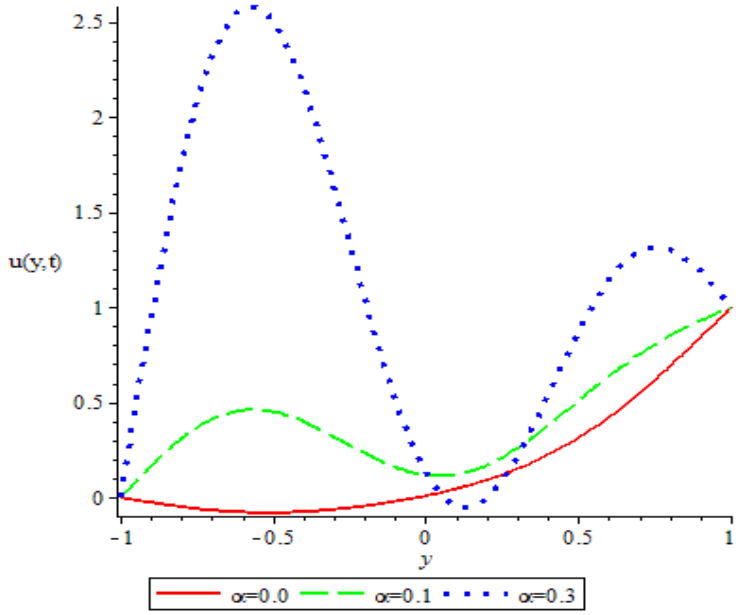

Figure 9: Effect of temperature dependent viscosity (α) on primary velocity profile $u(y,t)$

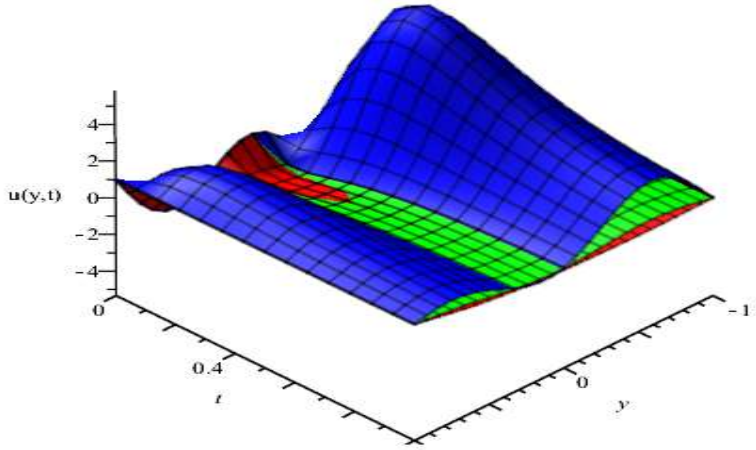

Figure 10: Effect of temperature dependent viscosity (α) on primary velocity profile $u(y,t)$ along distance y and time t.

(α) =0.0(red), (α) =0.1(green) and (α) =0.3(blue)

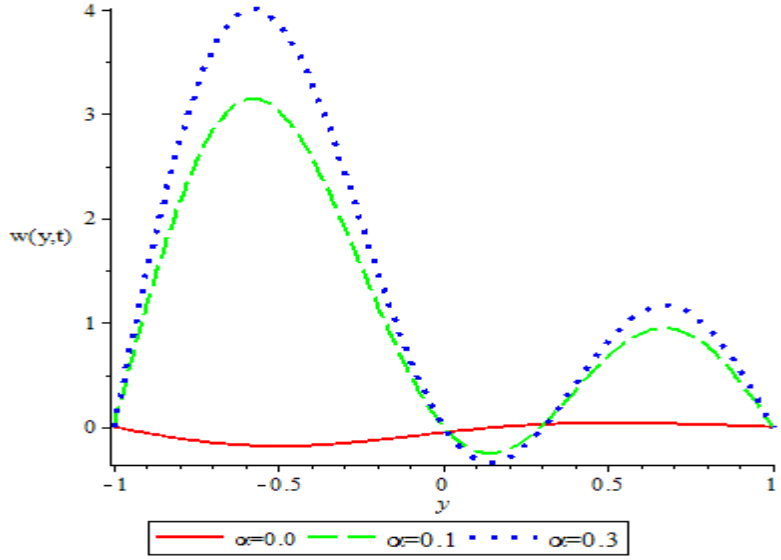

Figure 11: Effect of temperature dependent viscosity (α) on secondary velocity profile $w(y,t)$

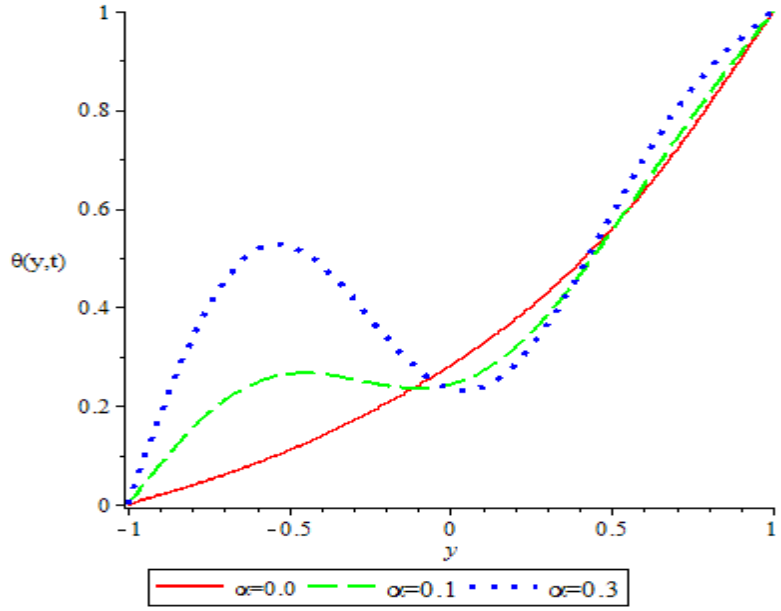

Figure 12: Effect of temperature dependent viscosity (α) on temperature profile $\theta(y,t)$

DISCUSSION OF RESULTS

Figure 2 displays the graph of temperature profile $\theta(y,t)$ for different values of radiation parameter (Ra). It is observed that temperature decreases as radiation parameter increases. Also, the temperature profile is observed to increase along distance.

Figure 3 shows the graph of primary velocity $u(y,t)$ for different values of suction parameter (S). It is evident that increase in suction parameter leads to decrease in primary velocity. It is also seen that primary velocity increases along distance y.

Figure 4 illustrates the effect of suction parameter (S) on the concentration profile $\phi(y,t)$ of the flow along distance and with time t. It is observed that concentration increases with time while increase in suction parameter leads to decrease in the fluid concentration.

Figure 5 presents the graph of temperature $\theta(y,t)$ for different values of Prandtl number (Pr). It is observed temperature increases along distance y and increase in Prandtl number leads to decrease in temperature.

Figure 6 depicts the effect of ion slip parameter (Bi) on secondary velocity $w(y,t)$ along y. it is seen that the

secondary velocity oscillates along distance y and increase in ion slip parameter leads to increase in secondary velocity.

Figure 7 displays the graph of secondary velocity $w(y,t)$ along distance and time for different values of ion slip parameter (Bi). It is observed that secondary velocity increases with time and oscillates along distance while increase in ion slip parameter leads to increase in secondary velocity.

Figure 8 depicts the graph of primary velocity $u(y,t)$ for different values of temperature dependent viscosity (α). It is observed that primary velocity is maximum when viscosity is temperature dependent as compared to when it is independent on temperature. Also, increase in temperature dependent viscosity leads to oscillation in primary velocity along distance y.

Figure 9 depicts the graph of primary velocity $u(y,t)$ for different values of temperature dependent viscosity (α). It is observed that primary velocity is maximum when viscosity is temperature dependent as compared to when it is independent on temperature. Also, increase in temperature dependent viscosity leads to oscillation in primary velocity along distance y.

Figure 10 presents the graph of primary velocity $u(y,t)$ for different values of temperature viscosity parameter (α) along distance and with time t. It is observed that primary velocity oscillates along distance y and increases with time.

Figure 11 depicts the graph of secondary velocity $w(y,t)$ for different values of temperature dependent viscosity (α). It is observed that primary velocity is maximum when viscosity is temperature dependent as compared to when it is independent on temperature. Also, increase in temperature dependent viscosity leads to oscillation in secondary velocity along distance y.

Figure 12 depicts the graph of temperature profile $\theta(y,t)$ for different values of temperature dependent viscosity (α). It is observed that temperature increases with increase in viscosity. Also, increase in temperature dependent viscosity leads to increase in temperature along distance y.

CONCLUSION

We have solved the equations governing the unsteady Couette flow of an electrically conducting incompressible fluid bounded by two parallel non conducting porous plates using the parameter expansion method and eigenfunction expansion technique. The effects of the dimensionless parameters as shown on the graphs were analyzed. From the results obtained, all the parameters have appreciable impact on the system since:

I. Reynolds number is observed to reduced primary velocity and temperature profiles respectively while secondary velocity profile is enhanced.
II. Hall parameter retards both primary and secondary velocities profiles while it enhances secondary velocity profile for unsteady state flow.
III. Temperature dependent viscosity enhances both temperature and primary velocity profiles respectively while variable pressure gradient is observed to reduce both primary and secondary velocities.

REFERENCES

1. Ajibade, A. O & Bichi, Y. A. (2019). Variable Fluid Properties and Thermal Radiation Effects of Natural Convection Couette Flow through a vertical Porous Channel. *Journal of Advances in Mathematics and Computer Science*, 2019; 2(4), 58 – 72.
2. Yusuf, A., Bolarin, G., Jiya, M., Aiyesimi, Y.M. & Okedayo, G. T (2018). Boundary Layer Flow of a Nanofluid in an Inclined Wavy Wall with Convective Boundary Condition.*Journal of Mathematics and Computer Science*, 2018; 1(2), 11-94.
3. E.O. Anyanwu, R.O. Olayiwola, M.D. Shehu and A.Lawal. Radiative Effects on Unsteady MHD Couette Flow through a Parallel Plate with Constant Pressure Gradient. *Asian Research Journal of Mathematics.* 2020; 16(9): 1-19.
4. Aiyesimi, Y. M., Yusuf, A. & Jiya, M. (2015). An Analytic Investigation of Convective Boundary Layer Flow of a Nanofluid Past a Stretching Sheet with Radiation.*Nigeria Association of Mathematical Physics*, 2015; 2(1), 12 – 35.
5. Laila R. & Marwat D. N. K. (2021). Nanofluid Flow in a convergind and Diverging Channel of Rectangular Heated Walls. *Ain Shams Engineering Journal* 2010; 12(4), 4023-4035.
6. Jiya M., Tsadu S & Yusuf A. (2015). Adomian Decomposition Method (ADM) Solution of Boundary Layer Flow Past a Streching Plate and Heat Transfer, Viscous Dissipation and Grashof Number. *Nigerian Journal of Mathematics and Applications.* 2015; 24(20) 165-175.
7. Chutia M. Tabendra N. D. & Pranob Y. C. (2017). Numerical Solution of Unsteady Hydromagnetic Couette Flow in a Rotating System Bounded by Porous Plates with Hall Effects. *International Journal of Computer Applications.* 2017; 71(2), 7-22.
8. Jana, M., Das, S. & Jana, R. N. (2012). Unsteady Couette flow through a porous medium in a rotating system. *Open Journal of Fluid Dynamics.* 2012; 2(2), 149-158.

9. Seth G. S., Ansari M. S. & Nandkeolyar, R (2010). Unsteady hydromagnetic Couette flow within porous plates in a rotating system. *Advanced Applied Mathematical Science.* 2010; 3(2), 2919-2932.
10. Seth G. S., Ansari M. S. & Nandkeolyar, R. (2011). Effects of rotation and magnetic field on unsteady Couette flow in a porous channel. *Journal of Applied Fluid Mechanics.* 2011; 4(2), 95-103.
11. Pramanik S. (2014). Casson fluid flow and heat transfer past an exponentially porous stretching Surfacein the presence of thermal radiation. *Ain Shams Engineering Journal* 2014; 5(2), 205-212.
12. Afikuzzaman, M. D., Ferdows, M. & Mahmud M. A (2015). Unsteady MHD Casson fluid flow through parallel plates with Hall currents. *Procedia Engineering*. 2015; 10(5), 287-293.
13. Sayed-Ahmed M.E, Attia H.A and Ewis K.M. Time dependent pressure gradient effect on unsteady MHD Couette flow and heat transfer of a Casson fluid. *Canadian Journal of Physics*. 2011; 3: 38-49.
14. Olayiwola R.O. Modelling and Simulation of Combustion Fronts in Porous Media. Journal of the Nigerian Mathematical Society 2015: 34, 1-10
15. Jana M, Das S, Jana RN. Unsteady Couette flow through a porous medium in a rotating system. *Open Journal of fluid dynamics.* 2012; 2: 149-158
16. Seth GS, Ansari MS and Nandkeolyar R. Effects of rotation and magnetic field on unsteady Couette flow in a porous channel. *Journal of applied fluid mechanics.* 2011; 4: 95-103.
17. Seth GS, Ansari MS and Nandkeolyar R. Unsteady hydromagnetic Couette flow within porous plates in a rotating system. *Advanced Applied Mathematical Science.* 2010; 3: 2919-2932.
18. Sharma PR, Yadav GR. Heat transfer through three dimensional Couette flow between a stationary porous plate bounded by porous medium and moving porous plates. *Ultra Sci. Phys. Sci.* 2005; 17(3): 351-360.
19. Sharma PR, Gaur YN, Sharma RP. Steady laminar flow and heat transfer of a non-Newtonian fluid through a straight horizontal porous channel in the presence of heat source. *Ind. J. Theo. Phys.* 2005; 53(1): 37-47.